11-1-2008

Identification of a functionally essential amino acid for Arabidopsis cyclic nucleotide gated ion channels using the chimeric AtCNGC11/12 gene

Joyce Baxter
University of Toronto

Wolfgang Moeder
University of Toronto

William Urquhart
University of Toronto

Dea Shahinas
University of Toronto

Kimberley Chin
University of Toronto

See next page for additional authors

Recommended Citation

Baxter, J., Moeder, W., Urquhart, W., Shahinas, D., Chin, K., Christendat, D., Kang, H., Angelova, M., Kato, N., & Yoshioka, K. (2008). Identification of a functionally essential amino acid for Arabidopsis cyclic nucleotide gated ion channels using the chimeric AtCNGC11/12 gene. *Plant Journal, 56* (3), 457-469. https://doi.org/10.1111/j.1365-313X.2008.03619.x

the plant journal

SEB SOCIETY FOR EXPERIMENTAL BIOLOGY

The Plant Journal (2008) **56**, 457–469 doi: 10.1111/j.1365-313X.2008.03619.x

Identification of a functionally essential amino acid for Arabidopsis cyclic nucleotide gated ion channels using the chimeric *AtCNGC11/12* gene

Joyce Baxter[1,2,†], Wolfgang Moeder[1,2,†], William Urquhart[1,2], Dea Shahinas[1,2], Kimberley Chin[1,2], Dinesh Christendat[1,2], Hong-Gu Kang[3], Magdalena Angelova[4], Naohiro Kato[4] and Keiko Yoshioka[1,2,*]

[1]*Department of Cell and Systems Biology, University of Toronto, 25 Willcocks Street, Toronto, ON M5S 3B2, Canada,*
[2]*Center for the Analysis of Genome Evolution and Function (CAGEF), University of Toronto, 25 Willcocks Street, Toronto, ON M5S 3B2, Canada,*
[3]*Boyce Thompson Institute for Plant Research, Tower Road, Ithaca, NY 14853, USA, and*
[4]*Department of Biological Sciences, Louisiana State University, Baton Rouge, LA 70803, USA*

Received 10 March 2008; revised 13 June 2008; accepted 25 June 2008; published online 14 August 2008.
*For correspondence (fax +1 416 978 5878; e-mail keiko.yoshioka@utoronto.ca).
†These authors contributed equally to this study.

Summary

We used the chimeric Arabidopsis cyclic nucleotide-gated ion channel AtCNGC11/12 to conduct a structure–function study of plant cyclic nucleotide-gated ion channels (CNGCs). AtCNGC11/12 induces multiple pathogen resistance responses in the Arabidopsis mutant constitutive expresser of PR genes 22 (*cpr22*). A genetic screen for mutants that suppress *cpr22*-conferred phenotypes identified an intragenic mutant, #73, which has a glutamate to lysine substitution (E519K) at the beginning of the eighth β-sheet of the cyclic nucleotide-binding domain in AtCNGC11/12. The #73 mutant is morphologically identical to wild-type plants and has lost *cpr22*-related phenotypes including spontaneous cell death and enhanced pathogen resistance. Heterologous expression analysis using a K^+-uptake-deficient yeast mutant revealed that this Glu519 is important for AtCNGC11/12 channel function, proving that the occurrence of *cpr22* phenotypes requires active channel function of AtCNGC11/12. Additionally, Glu519 was also found to be important for the function of the wild-type channel AtCNGC12. Computational structural modeling and *in vitro* cAMP-binding assays suggest that Glu519 is a key residue for the structural stability of AtCNGCs and contributes to the interaction of the cyclic nucleotide-binding domain and the C-linker domain, rather than the binding of cAMP. Furthermore, a mutation in the α-subunit of the human cone receptor CNGA3 that causes total color blindness aligned well to the position of Glu519 in AtCNGC11/12. This suggests that *AtCNGC11/12* suppressors could be a useful tool for discovering important residues not only for plant CNGCs but also for CNGCs in general.

Keywords: CNGC, cyclic nucleotide-gated ion channel, pathogen resistance, *cpr22,* Arabidopsis.

Introduction

Cyclic nucleotide-gated ion channels (CNGCs) are non-selective cation channels which were first discovered in retinal photoreceptors and olfactory sensory neurons (Zagotta and Siegelbaum, 1996; Zufall *et al.*, 1994). So far, six CNGC channel genes have been found in mammalian genomes and named *CNGA1–4* and *CNGB1* and *-3* (Kaupp and Seifert, 2002). Although when expressed heterologously, CNGA subunits form functional homomeric channels, the native channels are thought to be heterotetrameric in structure (Kaupp and Seifert, 2002; Zhong *et al.*, 2003). The structure of each subunit is similar to that of the voltage-gated outward rectifying K^+-selective ion channel (Shaker) proteins, including a cytoplasmic N-terminus, six membrane-spanning regions (S1–S6), a pore domain located between S5 and S6, and a cytoplasmic C-terminus (Zagotta and Siegelbaum, 1996). In contrast, CNGCs are opened by the direct binding of cyclic nucleotides (CN), such as cAMP and cGMP (Fesenko *et al.*, 1985). The CN-binding domain

(CNBD) of CNGCs is located at the cytoplasmic C-terminus and exhibits significant sequence similarity to that of protein kinase A, protein kinase G and CAP, the catabolite activator protein of *Escherichia coli* (Bridges *et al.*, 2005). The cytoplasmic C-terminus contains a CNBD and a C-linker region, which connects the CNBD to the pore domain. Important functional features of CNGCs have been extensively studied in animal systems and it has been suggested that the subunit composition of the respective channel complex is an important determinant for functional features such as ligand sensitivity, selectivity and gating. (Kaupp and Seifert, 2002).

On the contrary, plant CNGCs have only recently been investigated. The first plant CNGC, HvCBT1 [*Hordeum vulgare* calmodulin (CaM)-binding transporter], was identified as a CaM-binding protein in barley (Schuurink *et al.*, 1998). Subsequently, several CNGCs were identified from Arabidopsis and *Nicotiana tabacum* (Arazi *et al.*, 1999; Köhler and Neuhaus, 1998; Köhler *et al.*, 1999). The completion of the Arabidopsis genome sequencing project revealed a large family of CNGC genes, consisting of 20 members (Mäser *et al.*, 2001). Considering that only six CNGC genes were found in mammalian genomes, the large size of this gene family in plants suggests diversity and importance in their physiological functions in plants (Talke *et al.*, 2003).

Based on bioinformatics analyses, it is suggested that the members of the Arabidopsis CNGC family can be categorized into four different groups (I–IV) of which group IV is further broken into two subgroups (IVA and IVB; Mäser *et al.*, 2001). Possible biological functions of Arabidopsis CNGCs in development as well as pathogen resistance have been reported (Ali *et al.*, 2007; Balague *et al.*, 2003; Borsics *et al.*, 2007; Chan *et al.*, 2003; Clough *et al.*, 2000; Frietsch *et al.*, 2007; Gobert *et al.*, 2006; Köhler *et al.*, 2001; Li *et al.*, 2005; Ma *et al.*, 2006; Sunkar *et al.*, 2000; Yoshioka *et al.*, 2006).

Previously, in order to investigate the pathogen resistance signaling pathways, we identified the Arabidopsis mutant constitutive expresser of PR (pathogenesis related) genes 22 (*cpr*22; Yoshioka *et al.*, 2001). *cpr22* falls into the category of lesion-mimic mutants and constitutively activates various defense responses, exhibits stunted growth with curly leaves and displays enhanced resistance to the oomycete pathogen *Hyaloperonospora parasitica* (isolates Emco5 and Emwa1) as well as the bacterial pathogen *Pseudomonas syringae* pv. *maculicola* ES4326 (Yoshioka *et al.*, 2001, 2006). *cpr22* is a semi-dominant mutation, and interestingly it is lethal in the homozygous state unless the plant is grown under high relative humidity (>90%, Yoshioka *et al.*, 2001). Recently, the *cpr22* mutation was identified as a 3-kb deletion that fuses two CNGC-encoding genes, *AtCNGC11* and *AtCNGC12*, to generate a novel chimeric gene, *AtCNGC11/12* (Yoshioka *et al.*, 2006). Based on genetic and molecular analyses, it is suggested that AtCNGC11/12, as well as AtCNGC11 and AtCNGC12, form cAMP-activated functional CNGCs and that the phenotype conferred by *cpr22* is attributable to the expression of *AtCNGC11/12*. Furthermore, it is also hypothesized that *AtCNGC11/12* could be a constitutive active form of *AtCNGC12* or generate the downstream signal of *AtCNGC12* constitutively.

Here, we conducted a genetic screen for mutants that suppress *cpr22* (*AtCNGC11/12*)-conferred phenotypes. One intragenic suppressor mutant, #73, which is morphologically identical to wild-type plants, was identified through this screening. Analysis of this mutation revealed a functionally important residue, glutamate (E) 519. Furthermore, computational analyses showed the importance of this residue for AtCNGC function through the interaction of the CNBD and the C-linker domain.

Results

Screening for suppressor mutants of cpr22

In the screen for suppressors of *cpr22*, we took advantage of the conditional lethal phenotype of *cpr22* homozygous plants under ambient humidity conditions [relative humidity (RH) 55–65%]. Homozygous *cpr22* seeds were mutagenized with ethyl methane sulfonate (EMS) and the plants which could survive under ambient humidity conditions were identified in the M_2 generation. Seventy-four mutants that survived under ambient conditions were obtained out of approximately 10 000 M_2 seeds. These 74 plants were classified into six groups based on morphology: group 1, identical to wild type; group 2, similar to wild type with wavy leaves; group 3, similar to *cpr22* heterozygous plants; group 4, more pronounced phenotype than *cpr22* heterozygous; group 5, identical to wild type with spontaneous lesion formation; and group 6, others comprising various phenotypes (Figure 1a). Suppressor #73 was found to be morphologically identical to the wild type, and thus fell into group 1 (Figure 1b). To confirm the *cpr22* (*AtCNGC11/12*) homozygosity of suppressor #73, a PCR-based marker analysis was conducted. As shown in Figure S1, suppressor #73 was homozygous for *AtCNGC11/12* and not a contaminant. Nevertheless, suppressor #73 is neither lethal nor shows HR-like spontaneous lesion formation and constitutive *PR-1* gene expression (Figure 1b,c). Pathogen resistance was evaluated using the oomycete pathogen *H. parasitica* isolate Emwa1 which is virulent for ecotype Wassilewskija (Ws, the background ecotype of *cpr22*). *cpr22* showed enhanced resistance to the virulent strain Emwa1 (Yoshioka *et al.*, 2006). As we predicted, suppressor #73 lost *cpr22*-mediated enhanced resistance to this pathogen (Table 1). Taken together, we have concluded that suppressor #73 lost all tested *cpr22*-related phenotypes.

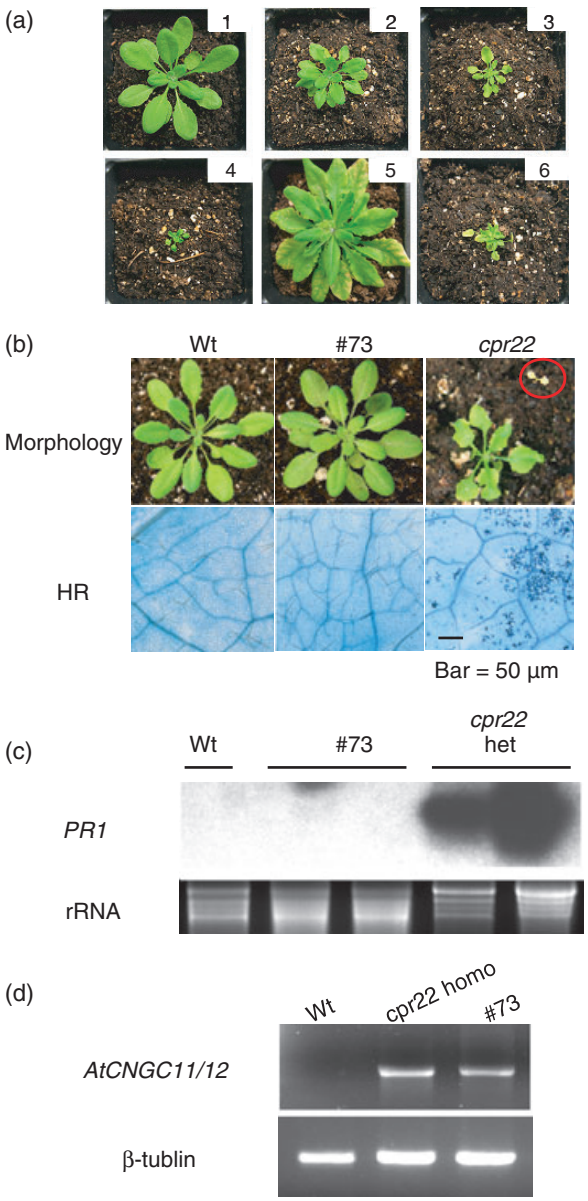

Figure 1. Characterization of suppressor mutants of *cpr22*.
(a) Morphological phenotypes of the six groups of *cpr22* suppressors. All plants are 5 weeks old: (1) group 1, identical to wild type (Wt); (2) group 2, similar to Wt plus wavy leaves; (3) group 3, similar to *cpr22* heterozygous plants; (4) group 4, more pronounced phenotype than *cpr22* heterozygous; (5) group 5, identical to Wt plus spontaneous lesion formation; and (6) group 6, others.
(b) Morphological phenotypes and spontaneous cell death formation of Wt, suppressor #73 and *cpr22*.
(c) Northern blot analysis for *PR-1* gene expression in Wt, suppressor #73 and *cpr22* (heterozygous).
(d) The RT-PCR analysis for the expression of *AtCNGC11/12* in Wt, suppressor #73 and *cpr22* (homozygous) plants (20 cycles).

Suppressor #73 is an intragenic suppressor of cpr22

To evaluate the genetic nature of the #73 mutation, a backcross with *cpr22* homozygous plants was carried out. As shown in Table 2, all B_1 (backcross, first generation) plants showed *cpr22* heterozygous-like phenotypes, suggesting that the #73 mutation is semi-dominant, just like the *cpr22* mutation itself. The following self-pollinated B_2 generation showed a segregation of 1:2:1 (wild-type like:*cpr22* heterozygous like:lethal), further confirming the semi-dominant nature of this mutation. Since *cpr22* is also a semi-dominant mutation, this result suggested that the #73 mutation might be an intragenic mutation. Therefore, the *cpr22* (*ATCNGGC11/12*) gene in suppressor #73 was sequenced. As expected, one nucleotide substitution, G to A was found at the cyclic nucleotide-binding domain (CNBD) in *AtCNGC11/12* that caused an amino acid substitution, glutamate 519 to lysine (E519K).

Table 1 Interaction phenotype with *H. parasitica* isolate Emwa1

		No. of plants[a]	
Plant	Total no. of plants	R	S
Wt	28	3	25
cpr22/CPR22	21	21	0
Suppressor #73	30	0	30

[a]Based on formation of sporangiophores; R, no formation; S formation.

Intragenic suppressor #73 defines a key residue for the induction of programmed cell death in Nicotiana benthamiana

Suppressor #73 lost all *cpr22*-associated phenotypes and carried one intragenic mutation in *AtCNGC11/12,* suggesting that the loss of phenotype is due to this mutation. However, considering that EMS treatment can create multiple mutations, it could not be ruled out that another mutation in the promoter region suppressed the expression of *AtCNGC11/12* with the E519K mutation. To confirm this, we have analyzed the expression of *AtCNGC11/12* with the #73 mutation (*AtCNGC11/12:E519K*) in the #73 mutant by semi-quantita-

Table 2 Morphological phenotype in progeny of crosses between #73 and homozygous *cpr22*

Plant line[a]	Total no.	Morphological phenotype					
		Wt	*cpr22*	Lethal	Hypothesis[b]	X^{2} [c]	*P*
cpr22 hetero	139	35	65	39	1:2:1	0.81	0.7 > *P* > 0.5
B_1[d]	13	0	13	0	0:1:0	–	–
B_2[e]	111	25	59	27	1:2:1	0.51	0.8 > *P* > 0.7

[a]#73 is the pollen accepting plant.
[b]Both *cpr22* and #73 are semi-dominant.
[c]Two degrees of freedom.
[d]Backcrossed first generation of #73 and *cpr22* homozygous plants.
[e]Backcrossed second generation of #73 and *cpr22* homozygous plants.

tive RT-PCR. As shown in Figure 1(d), *AtCNGC11/12:E519K* is expressed in #73 at a comparable level to *AtCNGC11/12* in *cpr22* homozygous plants. Next, we created the same point mutation (E519K) in *AtCNGC11/12* by site-directed mutagenesis and tested its ability to induce programmed cell death (PCD) in *N. benthamiana* using *Agrobacterium tumefaciens*-mediated transient expression. Previously, we have reported that transient expression of *AtCNGC11/12,* but not the wild-type genes, *AtCNGC11* or *-12*, induced PCD using this method (Urquhart *et al.*, 2007; Yoshioka *et al.*, 2006). As shown in Figure 2(a), transient expression of *AtCNGC11/12* induced clear PCD, whereas *AtCNGC12*, empty vector and *Agrobacterium* itself did not. As expected, expression of point-mutated *AtCNGC11/12:E519K* did not induce PCD in *N. benthamiana*, confirming the importance of E519 for induction of PCD (Figure 2a). The expression of all genes was confirmed by green fluorescence of green fluorescent protein (GFP) which was fused to the C-terminus of each protein, as well as by RT-PCR (Figure 2b,c). It should be noted that we have already shown that the fusion of GFP at the C-terminal did not alter the function of these proteins (Urquhart *et al.*, 2007).

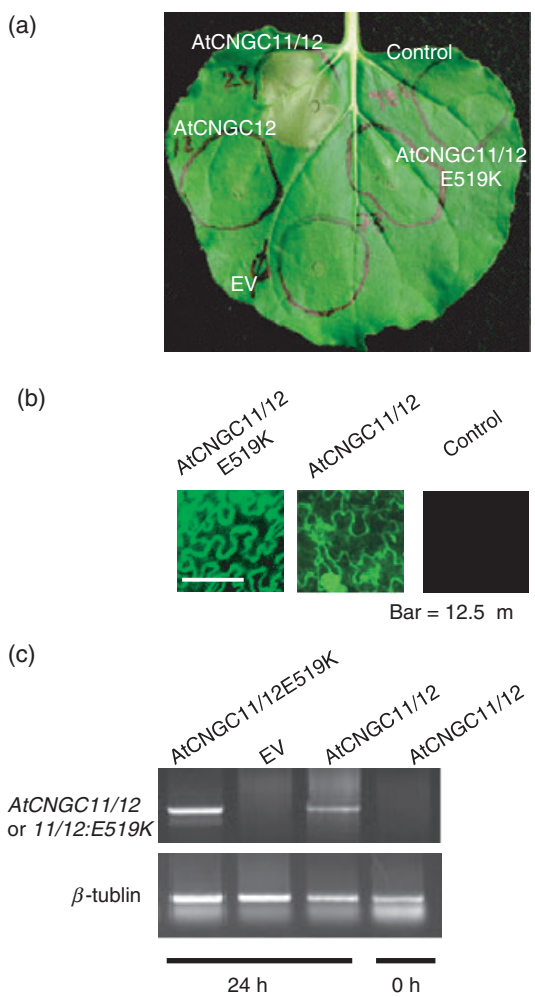

Figure 2. Induction of programmed cell death by AtCNGC11/12 was suppressed by the E519K substitution. EV, empty vector; control, *Agrobacterium* without vectors.
(a) Induction of cell death in *Nicotiana benthamiana* 48 h after *Agrobacterium*-infiltration.
(b) Expression of *AtCNGC11/12:GFP* and *AtCNGC11/12:E519K:GFP* in *N. benthamiana* leaves at 32 h post-infiltration (hpi) was monitored by fluorescence microscopy.
(c) The RT-PCR analysis of leaf discs from *N. benthamiana* leaves expressing *AtCNGC11/12:E519K:GFP*, empty vector or *AtCNGC11/12:GFP* at 24 hpi and *AtCNGC11/12:GFP* at 0 hpi. β-tubulin served as a loading control (20 cycles).

E519K mutation does not cause a significant alteration in subcellular localization

Since E519 locates to the cytosolic C-terminal area, it is unlikely to affect the subcellular localization of this protein significantly. However, to rule out this possibility, we compared the localization of this mutant protein with that of AtCNGC12. For this analysis, we employed transient expression analysis in Arabidopsis protoplasts using GFP fusions of AtCNGC12, AtCNGC11/12, AtCNGC11/12:E519K, the plasma membrane localized protein SYP123 and cytosolic GFP (Uemura *et al.*, 2004). As shown in Figure 3, the localization patterns of all three CNGC proteins were similar and no significant difference was observed. The localization pattern of these three proteins resembles that of SYP123, not cytosolic GFP. Previously our group showed that AtCNGC11, -12 and AtCNGC11/12 localized in the plasma membrane in yeast cells (Urquhart *et al.*, 2007). Thus, these data support our previous observation in yeast cells. We noticed the transfection efficiencies of AtCNGC-GFP plasmids were extremely low. In our hands, the average transfection rate of Arabidopsis protoplasts is approximately 25%. In contrast, fewer than 3% of protoplasts showed clear GFP signals with AtCNGCs in this study. This indicates that accumulation of the AtCNGCs may be restricted, or the turnover of AtCNGCs may be fast.

Based on this analysis, we concluded that the E519K mutation does not alter subcellular localization significantly. Thus, E519K must affect other aspect(s) of AtCNGC11/12 to abolish the AtCNGC11/12-mediated phenotypes.

#73 mutation (E519K) abolished ion channel function in a yeast mutant

It has been suggested that AtCNGC11, -12 and AtCNGC11/12 function as cAMP-activated K^+ channels as well as Ca^{2+} channels in yeast mutants (Urquhart *et al.*, 2007; Yoshioka *et al.*, 2006). The above analyses indicated that the #73 mutation suppressed the ability of AtCNGC11/12 to induce *cpr22*-related phenotypes. However, it is not clear whether E519K affects its channel function itself or the constitutive active nature of AtCNGC11/12 by influencing the transmission of downstream signals. To address this point, we

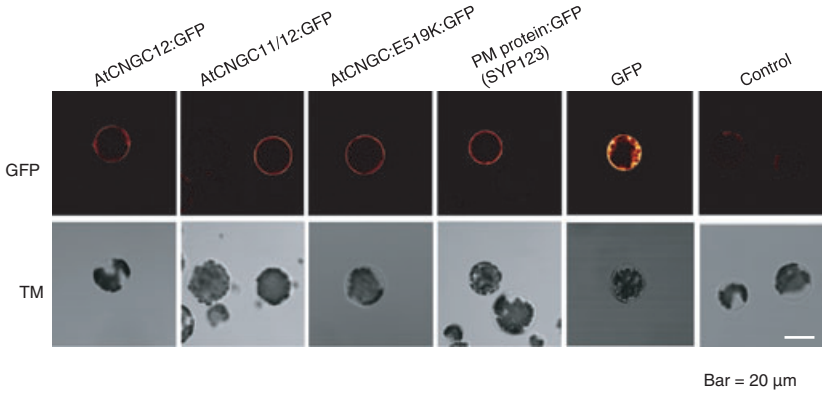

Figure 3. AtCNGC12, AtCNGC11/12 and AtCNGC11/12:E519K are localized at the plasma membrane.
Subcellular localization was monitored by fluorescence microscopy after protoplast transfection. SYP123 was used as a control for a plasma membrane localized protein. Green fluorescent protein alone was used as a control for cytoplasm localization. The fluorescence images were presented as glow-over/under images in which high-intensity pixels appeared in orange-to-white colors. GFP, green fluorescent protein; TM, transmitted light.

employed a yeast growth assay to evaluate the channel function of AtCNGC11/12:E519K. Previously, we have shown that Ca^{2+} is important for induction of PCD (Urquhart *et al.*, 2007). However, the assay we used for the Ca^{2+} channel function was not suitable for quantitative analysis. Therefore, in this study we have used the K^+-uptake-deficient yeast mutant strain CY162 to show clear growth kinetics of yeast. The K^+-uptake-deficient yeast mutant CY162 lost two major K^+ channels, *trk1* and *trk2*, and consequently cannot grow well in low-K^+ medium (Leng *et al.*, 1999). The CY162 transformed with the empty vector did not grow well in low-K^+ medium, whereas the mutants carrying *AtCNGC11/12* or the *AtCNGC12* wild-type gene grew well, suggesting that these proteins function as K^+ channels in yeast (Figure 4a). On the contrary, the yeast CY162 carrying *AtCNGC11/12:E519K* grew as poorly as the empty vector control, indicating that the E519K mutation attenuates the K^+ channel function of AtCNGC11/12. Based on semi-quantitative RT-PCR, the expression levels of *AtCNGC11/12* and *AtCNGC11/12:E519K* in yeast are comparable (Figure S2). This result suggests that the #73 mutation causes destruction of the channel function itself, not the constitutive active nature of AtCNGC11/12.

This result led us to analyze the effect of this E519K mutation in wild-type AtCNGC12 in order to evaluate whether this residue is important not only for channel function of the chimeric protein but also for its wild-type protein. For this analysis *AtCNGC12:E527K* (the position of E519 in AtCNGC11/12 is E527 in AtCNGC12) was constructed. Strikingly, like *AtCNGC11/12:E519K*, the expression of *AtCNGC12:E527K* also failed to rescue the deficiency of this yeast mutant (Figure 4b). Again, the expression level of the *AtCNGC12:E527K* in yeast was confirmed by RT-PCR (Figure S2). Taken together, these results suggest that the E519K mutation causes disruption of the channel function itself, not the constitutive active nature of AtCNGC11/12, and this residue is important not only for AtCNGC11/12, but also for the function of the wild-type protein AtCNGC12.

Additionally, this result also indicates that the occurrence of the *cpr22* phenotypes requires active channel function.

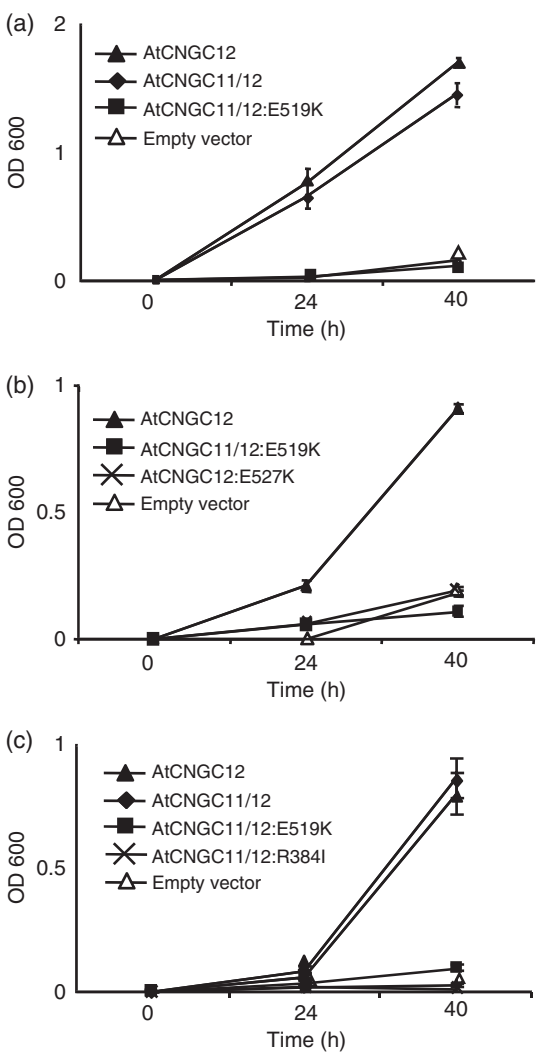

Figure 4. Yeast complementation analysis using the K^+-uptake-deficient mutant CY162.
(a) *AtCNGC12* and *AtCNGC11/12*, but not *AtCNGC11/12:E519K*, complemented K^+-uptake deficiency of CY162.
(b) The wild-type *AtCNGC12* gene with the same mutation as suppressor #73, *AtCNGC12:E527K* also did not rescue the deficiency of CY162.
(c) *AtCNGC11/12:R384I* did not rescue the deficiency of CY162.

Glutamate 519 (527 in AtCNGC12*) is highly conserved among plant CNGCs*

Sequence comparisons have demonstrated that the CNBDs of the 20 Arabidopsis CNGCs clustered in the same pattern as the full-length sequences (Bridges *et al.*, 2005; Kaplan *et al.*, 2007; Mäser *et al.*, 2001). The only exception to this is AtCNGC12 which has a remarkably different CNBD sequence. It not only deviates from those sequences in group I, to which AtCNGC12 belongs, but also from those in other groups, suggesting an intriguing uniqueness in regulation of this particular subunit. Nevertheless, E519 in AtCNGC11/12 (E527 in AtCNGC12) is well conserved among 16 out of 20 Arabidopsis CNGCs, including AtCNGC12 (Table 3: listing only group I of the AtCNGCs). Furthermore, this conservation is also observed in CNGCs of other plant species such as rice (*Oryza sativa*), tobacco (*Nicotiana tabacum*), barley (*H. vulgare*) and bean (*Phaseolus vulgaris*) (Table 3). The high degree of conservation of this amino acid presumably reflects the functional importance of this residue.

Computational structural prediction suggests importance of E519 for the interaction between the C-linker domain and the CNBD

Since the E519K mutation disrupts channel function, a computational analysis of the three-dimensional structure of the cytoplasmic C-terminal region was conducted in order to predict the role of this residue in channel structure. Recently, the structure of the cytoplasmic C-terminal region of a hyperpolarization-activated cyclic nucleotide-modulated channel, HCN2, that contains both the C-linker and the CNBD, has been solved by X-ray crystallography (Zagotta *et al.*, 2003; Protein Data Bank (PDB) ID: 1Q50). HCN2 is also activated by the direct binding of cyclic nucleotide monophosphate (cNMP) and its intracellular C-terminal regions exhibits high similarity to those of CNGCs. Therefore to create our model of AtCNGC11/12:E519K and AtCNGC11/12 we used this crystal structure as a template. Based on our model, the C-linker domain of AtCNGC11/12 (the same as AtCNGC12) has six α-helices, and the CNBD consists of four α-helices and two anti-parallel β sheets consisting of four strands each, creating a β-roll between the first and second helix (Figure 5a). Overall our model of the CNBD portion agrees well with previously reported models of the CNBD (Bridges *et al.*, 2005; Hua *et al.*, 2003; Kaplan *et al.*, 2007). Based on X-ray crystallographic structures of the HCN2 CNBD bound with cNMPs, it is suggested that cNMPs are bound inside of the β-roll and interact with the C-helix (Zagotta *et al.*, 2003). This was also suggested by Hua *et al.* (2003) using their AtCNGC2 model. Based on our model, E519 is located at the beginning of the eighth β-sheet in the CNBD (Figure 5a). According to the crystal structure of the CNBD of HCN2 in the presence of cAMP, cAMP binds in the anti-configuration between the β-roll and the third helix (C-helix) of the CNBD. Interestingly, our model showed that the side chain of the E519 faces away from the interior of the cNMP-binding pocket formed by the β-roll, indicating that the E519K mutation may not affect cNMP binding. This observation was also confirmed by modeling against the

Table 3 Alignment of the area of E517 with various CNBDs

Gene[a]	Origin[b]	Alignment[c]
AtCNGC 1	Arabidopsis	FCGEELLTWALDPHSSSNLPISTRTVRALM**E**VEAFALKADDLKFVASQFRRLHSKQLRHT
AtCNGC 10	Arabidopsis	FCGEELLTWALDPHSSSNLPISTRTVRALM**E**VEAFALKADDLKFVASQFRRLHSKQLRHT
AtCNGC 13	Arabidopsis	FCGEDLLTWALDPQSSSHFPISTRTVQALT**E**VEAFALAADDLKLVASQFRRLHSKQLQHT
AtCNGC 3	Arabidopsis	FCG-DLLTWALDPLSS-QFPISSRTVQALT**E**VEGFLLSADDLKFVATQYRRLHSKQLRHM
AtCNGC 11	Arabidopsis	SCG-DLLTWALYSLSS-QFPISSRTVQALT**E**VEGFVISADDLKFVATQYRRLHSKQLQHM
AtCNGC 12	Arabidopsis	ICGELLFNGSR-------KPTSTRTVMTLT**E**VEGFILLPDDIKFIASHLNVFQRQKLQRT
AtCNGC 11(Ws)	Arabidopsis	FCG-DLLTWALDPLSS-QFPISSRTVQAWT**E**VEGFLLSADDLKFVVTQYRRLHSKQLRHM
AtCNGC 12(Ws)	Arabidopsis	ICGELLFNGSR-------LPTSTRTVMTQT**E**VEGFILLPDDIKFIASHLNVFQRQKLQRT
OsCNGC 1a	Rice	FCGEELLTWALDPTSASNLPSSTRTVKTLS**E**VEAFALRADDLKFVATQFRRLHSKQLQHT
NtCBP4	Tobacco	FCGEELLTWALDPAAVSNLPSSTRTVKTLS**E**VEAFVLRADDLKFVATQFRKLHSKQLQHT
NEC1	Barley	FCGEELLTWALDPAAVSNLPSSTRTVKTLS**E**VEAFVLRADDLKFVATQFRKLHSKQLQHT
PvCNGC-C	Bean	FCGEELITWALDPHSSSNLPTSTRTVMTQT**E**VEGFILLPDDIKFIASHLNVFQRQKLQRT
CNGA 1	Human	ISILNIKGSKA-------GNRRTANIKSIG**Y**SDLFCLSKDDLMEALTEYPDAKTMLEEKG
CNGA 3	Human	ISILNIKGSKS-------GNRRTANIRSIG**Y**SDLFCLSKDDLMEALTEYPEAKKALEEKG
HCN 2	Human	ICLLTR-------------GRRTASVRADT**Y**CRLYSLSVDNFNEVLEEYPMMRRAFTVAI

[a]NCBI Accession #,AtCNGC1:AAK43954, AtCNGC10:AAF73128, AtCNGC13:AAL27505, AtCNGC3:CAB40128, AtCNGC11:AAD20357, AtCNGC12:AAd23055, AtCNGC11(Ws):EU541496, AtCNGC12(Ws):EU541495, OsCNGC1a:BAD29689, NtCBP4:AAF33670, NEC1:AAY58314,PvCNGC-C:AAN65366.1, CNGA1:NP_000078, CNGA3:NP_001289 (isoform 1), HCN2:NP_001185, Ws: ecotype Ws.

[b]Arabidopsis: Arabidopsis thaliana, Rice: Oryza sativa, Tobacco: Nicotiana tobacum, Barley: Hordeum vulgare, Bean: Phaseolus vulgaris. Human:Homo sapiens.

[c]E517 and aligned aa with E517 were indicated by bold.

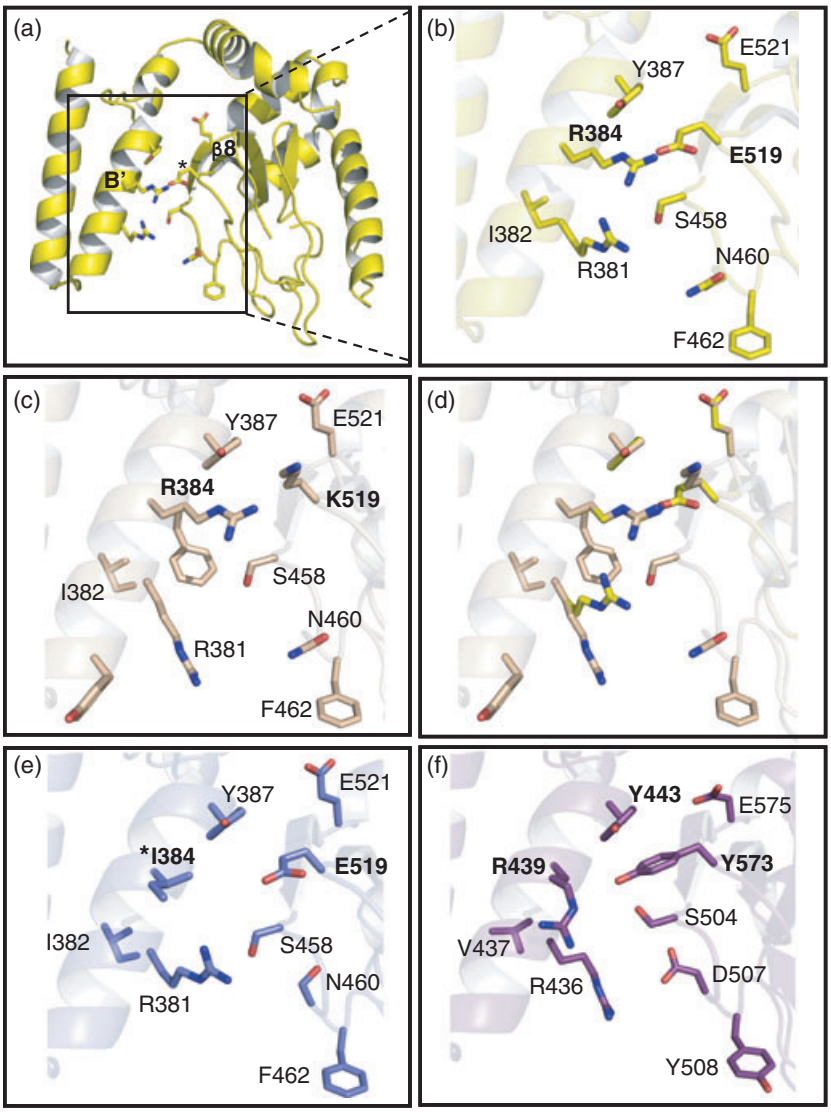

Figure 5. Computational structural modeling of the cytoplasmic C-terminal region of AtCNGC11/12, AtCNGC11/12:E519K, AtCNGC11/12:R384I and human CNGA3.
The protein sequence from the residues after the sixth transmembrane domains (S350 to A641 in AtCNGC11/12; EU541497) was modeled to the crystallized HCN2 structure (PDBID:IQ50, Zagotta *et al.*, 2003).
(a) Ribbon diagram of the cytoplasmic C-terminal region of AtCNGC11/12. The asterisk indicates E519.
(b) Close-up of the indicated area of (a).
(c) Close-up of the same area of AtCNGC11/12:E519K.
(d) Superimposition of (b) and (c).
(e) Close-up of the same area of AtCNGC11/12:R384I. The asterisk indicates mutated residue.
(f) Close-up of the same area of CNGA3.

crystallized structure of the CNBD of bovine cAMP-dependent protein kinase A (RI α; data not shown). Rather than affecting cAMP binding, E519 probably influences the interaction between the CNBD and the C-linker domains through possible interactions with several surrounding residues in the second α-helix (B'), of the C-linker domain. Negatively charged E519 seems to interact with a positively charged arginine residue (R384) by forming a salt bridge (Figure 5b). It has been suggested that the interaction between the CNBD and the C-linker domain is important for intrasubunit interactions as well as inter-subunit interactions in animal CNGCs (Zagotta *et al.*, 2003). As shown in Figure 5(c), replacing the negatively charged E519 with a positively charged lysine (E519K) would destroy this salt bridge. The superimposition of the modeled domains of AtCNGC11/12:E519K and AtCNGC11/12 clearly indicates that this interaction is disturbed by the E519K mutation (Figure 5d). Thus, it is hypothesized that E519K caused loss of channel function mainly through disruption of this E519-dependent salt bridge and not through the interference of cNMP binding.

To support this hypothesis we analyzed the physical interaction of the CNBD of AtCNGC11/12 or AtCNGC11/12:E519K and cAMP. Previously, we have shown that cAMP, but not cGMP, enhanced the activation of AtCNGC11/12 as well as AtCNGC12 in a yeast complementation assay (Yoshioka *et al.*, 2006). Thus we conducted an *in vitro* binding assay with cAMP-agarose. Histidine (His)-tagged CNBDs of *AtCNGC11/12* (the same as *AtCNGC12*) and AtCNGC11/12:E519K were expressed and soluble proteins were extracted and purified. The binding with cAMP was tested using cAMP-agarose, and proteins that bind to cAMP were detected by western blot analysis using an α-His antibody. The CNBD of AtCNGC11/12 bound to the cAMP

resin, whereas a negative control (aconitase) that does not possess a CNBD (Moeder *et al.*, 2007) did not show significant binding (Figure 6). The amount of protein binding to the cAMP-resin was not altered by the E519K mutation, suggesting that E519K does not affect cAMP binding (Figure 6). This result is consistent with our computational modeling prediction. Previously Hua *et al.* (2003) and Kaplan *et al.* (2007) reported structural models of the CNBDs of Arabidopsis CNGC2 and CNGC6, respectively, and identified several residues possibly interacting with cAMP. As we expected, none of these residues aligned with E519 (data not shown).

Taken together, we hypothesize that E519 is essential for CNGC function by influencing intrasubunit interaction between the C-linker and the CNBD. This interaction is probably mediated through a salt bridge formed between E519 and R384, and the E519K mutation disrupts this salt bridge resulting in a loss of channel function.

A mutation of R384 causes the same disruption of channel function

To further test the importance of E519, we constructed *AtCNGC11/12:R384I*. If our hypothesis is correct, the substitution from arginine (strong basic) to isoleucine (neutral) should disrupt a possible salt bridge formed with glutamate E519 (acidic) (Figure 5e). We predicted that this disruption would result in a loss of channel function, similar to that seen in the E519K mutation. Indeed, the expression of *AtCNGC11/12:R384I* in *N. benthamiana* failed to induce PCD, suggesting the disruption of biological function (Figure 7a). Transcription and translation of *AtCNGC11/12:R384I* in *N. benthamiana* were confirmed by RT-PCR as well as GFP expression (Figure 7a,b). Furthermore, we conducted K^+-yeast mutant complementation analysis using *AtCNGC11/12:R384I*. As expected, the yeast expressing *AtCNGC11/12:R384I* did not grow well in low-K^+ medium, similar to that of *AtCNGC11/12:E519K*-expressing yeast, suggesting the disruption of channel function by this mutation (Figure 4c). Again the expression level of *AtCNGC11/12:R384I* in yeast was confirmed by RT-PCR (Figure S2). Another suppressor mutant with a mutation in the CNBD was isolated from our suppressor screen. Modeling showed that the mutated residue is not involved in the formation of a salt bridge with the C-linker. Interestingly, this mutant maintained its channel function in yeast (data not shown). Thus, E519 is an essential residue for the channel function to stabilize the intrasubunit interaction, probably due to the formation of a salt bridge with arginine 384 (R384) in the C-linker domain. The disruption of this salt bridge probably causes instability of intrasubunit interactions and leads to a loss of function of this channel.

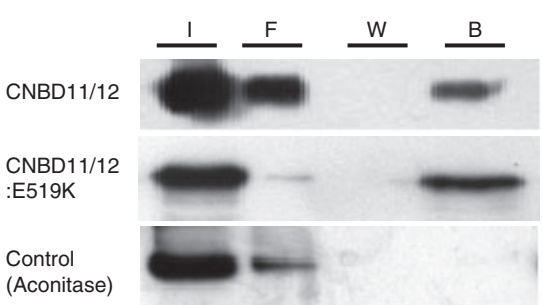

Figure 6. The cAMP binding assay with the cyclic nucleotide-binding domain (CNBD) region of AtCNGC11/12 (same as AtCNGC12), AtCNGC11/12:E519K under high-stringency conditions (500 mM NaCl).
Both proteins were expressed as a fusion protein with a histidine (His)-tag and purified by a nickel column. Western blot analysis with an α-His-tag antibody was conducted to detect the fusion protein. Legend: input (I), flow-through (F), first wash (W), and protein bound to cAMP resin (B). Aconitase fused with a His-tag served as a negative control.

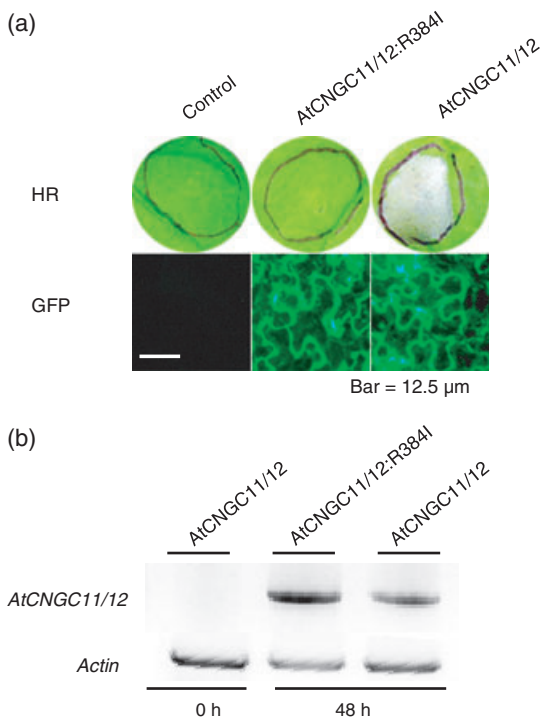

Figure 7. AtCNGC11/12:R384I lost the ability to induce programmed cell death in *Nicotiana benthamiana*.
(a) Cell death formation in *N. benthamiana* at 48 h post-infiltration (hpi). Expression of AtCNGC11/12 and AtCNGC11/12:R384I was monitored by fluorescence microscopy at 36 hpi.
(b) Reverse-transcriptase-PCR of leaf discs from *AtCNGC11/12*-expressing *N. benthamiana* leaves 0 hpi and from *AtCNGC11/12* or *AtCNGC11/12:E519K*-expressing *N. benthamiana* leaves 48 hpi (27 cycles). Actin served as a loading control.

Glutamate 519 aligns well with tyrosine 573 in CNGA3, which is essential for human vision

The CNGCs were first discovered in retinal photoreceptors and olfactory sensory neurons (Zagotta and Siegelbaum,

1996; Zufall *et al.*, 1994). *CNGA3* encodes the α-subunit of the cone photoreceptor cGMP-gated channels. It has been reported that a mutation in this gene causes achromatopsia. Knockout mice showed complete absence of physiologically measurable cone function (Biel *et al.*, 1999). Furthermore, Wissinger *et al.* (2001) conducted the first comprehensive screen for *CNGA3* mutations in human families with hereditary cone photoreceptor disorders from which 38 new *CNGA3* mutations were discovered. These novel mutations include missense mutations, as well as substitutions at the transmembrane domains S1 and S2, S4 and in the cGMP-binding domain (e.g. tyrosine (Y)573). The E519 in AtCNGC11/12 (E527 in AtCNGC12) aligned well with Y573 in the cGMP-binding domain of CNGA3 (Table 3). This Y573 is well conserved among the various CNG channels in vertebrate photoreceptors and the olfactory epithelium, as well as in CNGCs in *Drosophila melanogaster* and *Caenorhabditis elegans*. The conservation of Y573 presumably reflects the functional importance of this amino acid position (Wissinger *et al.*, 2001). A Y to cysteine (C) substitution in this position caused complete achromatopsia in humans, suggesting a loss of channel function. To see the alignment of not only the primary, but also the tertiary structure, we have generated a computational model of the CNBD of CNGA3 using the crystal structure of the cytoplasmic C-terminal region of HCN2. Based on this analysis, Y573 locates in the same position as E519 in AtCNGC11/12 (Figure 5f). Although a salt bridge between two domains through this residue does not exist in this CNGA3 model, hydrogen-bonding interactions between Y573 in the CNBD and residues in the C-linker domain are likely. Considering the conservation of structural topology, it is possible that Y573 in CNGA3 plays an equivalent role to E519 in AtCNGC11/12. This suggests an interesting structural conservation between animal and plant CNGCs, and at the same time the possibility that screening of AtCNGC11/12 suppressor mutants could be used to predict essential residues, not only for plant CNGCs but also for animal CNGCs.

Discussion

Plants possess a myriad of ion channels to regulate their physiological homeostasis, control development and transmit signals in reaction to numerous stimuli. Among them, the CNGC family and the five groups of shaker-like potassium channels possess a clear cNMP-binding domain, indicating their regulation by this universal second messenger. The cNMPs were discovered almost 50 years ago through the study of adrenaline and glucagons in dog liver (Rall *et al.*, 1957). Since then the importance of cNMPs in various physiological responses has been shown and these small second messengers are well studied in animals (Newton and Smith, 2004). On the other hand, over the years the existence of cNMPs and their function in plants has been a controversial topic. However, in the last decade significant progress has been made and some roles of cNMPs and their downstream targets were gradually revealed (Kaplan *et al.*, 2007; Newton and Smith, 2004). For example, cNMPs have demonstrated developmental roles in pollen growth and reorientation, as well as auxin-induced adventitious rooting (Moutinho *et al.*, 2001; Pagnussat *et al.*, 2003). Frietsch *et al.* (2007) recently reported solid evidence for a role of AtCNGC18 in polarized tip growth of pollen, further indicating the function of cNMPs in pollen development. The importance of cNMPs and their connection with CNGCs in pathogen resistance has also been reported by several research groups (Ali *et al.*, 2007; Balague *et al.*, 2003; Clough *et al.*, 2000; Durner *et al.*, 1998; Jiang *et al.*, 2005; Jurkowski *et al.*, 2004; Rostoks *et al.*, 2006; Yoshioka *et al.*, 2006).

Previously, we identified the Arabidopsis mutant *cpr22* that exhibits multiple pathogen resistance responses constitutively (Yoshioka *et al.*, 2001). In *cpr22* a 3-kb deletion in a cluster of CNGCs on chromosome 2 created the novel chimeric AtCNGC11/12 (Yoshioka *et al.*, 2006). Further characterization suggested that the expression of *AtCNGC11/12* causes the *cpr22* phenotypes. AtCNGC11/12 could be a constitutive active form of AtCNGC12 or activate downstream signaling of AtCNGC12 constitutively to induce the *cpr22* phenotypes, including HR-like programmed cell death (Urquhart *et al.*, 2007; Yoshioka *et al.*, 2006). Here, in order to understand the structural basis of AtCNGC11/12, we conducted a genetic screen for *cpr22* suppressor mutants. Through this screening, we identified mutant #73, which possesses a E519K substitution in the CNBD in AtCNGC11/12. This substitution caused loss of channel function and consequently suppressed *AtCNGC11/12*-mediated phenotypes.

In animal CNGCs it has been reported that the purine ring of cNMPs interacts with particular residues in the C-helix of the CNBD through hydrogen bonds, and the ribofuranose moiety of cNMPs stabilizes its binding in the β-roll in the CNBD (Goulding *et al.*, 1994; Kaupp and Seifert, 2002; Zagotta and Siegelbaum, 1996). Residues that may interact with cNMPs have been identified by mutational analysis using animal CNGCs (Kaupp and Seifert, 2002). Additionally, using the CNBD of plant CNGCs, computational modeling and alignment studies identified residues that may bind to cNMPs (Hua *et al.*, 2003; Kaplan *et al.*, 2007). Glutamate 519 did not align with any of these residues, suggesting that the loss of channel function is not due to the alteration of binding to cNMPs. Our *in vitro* cAMP-binding assay and computational modeling further supported this notion.

Based on our computational prediction, we proposed that there is an important interaction between E519 and R384 which keeps conformational stability of the channel through the interaction of the second α-helix (B′) and the eighth β-sheet from the C-linker and the CNBD, respectively. In this

scenario, the substitution of E519 to K519 led to a repulsion of R384, which consequently loosened the interaction between the α-helix B′ and the eighth β-sheet. Supporting this model, an R384I substitution also disrupted this interaction by breaking the R384–E519 salt bridge, resulting in a complete loss of PCD in *N. benthamiana* and of channel function in yeast. To further explore this model, two additional mutants, R384E and R384D both in the E519K background, were generated to test whether the interaction between a basic and an acidic residue in this position can restore its channel function. However, a clear restoration of HR/PCD development in *N. benthamiana* was not observed, which suggests that there are other minor interaction(s) required for the recovery of channel function (data not shown). For example, based on our model, Y387 has a favorable position to mediate the distribution of electronegativity in order to buffer the interactions between negatively and positively charged residues, such as R384 or K519. Y387 may play a role in the stable interaction between the C-linker and the CNBD. Alternatively, if the restoration by R384E and R384D is only partial, the assay method for restoration of channel function (i.e. HR/PCD development in *N. benthamiana*) may not be sensitive enough and consequently the restoration would not be detected. Further studies utilizing site-directed mutagenesis will reveal more details of the interaction between the C-linker and the CNBD.

Interestingly, Craven and Zagotta (2004) identified a glutamate in the second β-strand of the CNBD of HCN2 and CNGA1, which has a strong interaction with an arginine in the B-helix of the C-linker forming an intrasubunit salt bridge. This salt bridge proved necessary for proper gating in the HCN2 channels. In CNGA1, this intrasubunit salt bridge affected channel activation by altering ligand specificity (Craven and Zagotta, 2004). Even though E519 is not at exactly the same position as the glutamate identified in the HCN2 and CNGA1 channels, the study also demonstrates a loss of channel function by disrupting just one amino acid interaction between these two domains.

Nevertheless, how the C-linker domain contributes to conformational rearrangements during channel gating is still not completely clear. Recently, several crystal structural analyses have suggested that a large conformational change in the C-linker domain occurs during channel gating (Craven and Zagotta, 2004; Johnson and Zagotta, 2001). This suggests the importance of this domain for channel activation. However, a detailed analysis of the conformational change, especially as a tetramer, is a difficult task. Furthermore, there is as yet no report regarding the subunit composition of plant CNGCs. In order to understand the role of the C-linker domain in plant CNGCs during gating, accumulation of more basic knowledge of this channel family in plants is required.

Through this study, we found that E519 aligns well with Y573 in human CNGA3. A mutation in Y573 causes achromatopsia in humans (Wissinger *et al.*, 2001). Although the functional analysis and biophysical characterization of this mutation in human CNGA3 has not been reported yet, given the fact that Y573 is highly conserved among various organisms it can be speculated that the Y573 position play a functionally important role. Since the tertiary structure is well conserved between plant and animal CNGCs, this indicates that the unique constitutive active nature of the AtCNGC11/12 channel could be used to identify functionally important residues in CNGCs in general through a suppressor screening. Further analyses on other intragenic suppressors are in progress.

Experimental procedures

Plant growth conditions

Arabidopsis thaliana plants were grown on Pro-Mix soil (Premier Horticulture Inc., http://www.premierhort.com/) in a growth chamber under ambient humidity as described by Silva *et al.* (1999). For the high-RH condition, 95% RH was applied. *Nicotiana benthamiana* plants were grown on the same soil in a greenhouse under a 14:10 h light:dark regimen at 25°C (day), 20°C (night) with 65% humidity.

Suppressor screening and identification of the #73 mutant

Approximately 10 000 *cpr22* homozygous seeds M_0 were mutagenized with 0.3% (v/v) EMS solution (Sigma-Aldrich, http://www.sigmaaldrich.com/) for 8 h at room temperature, followed by rinsing more than 15 times in water. The M_0 seeds were grown under high humidity (RH >90%) for M_1 plants. The M_2 seeds were collected and then screened for suppressor plants under normal humidity. Suppressor #73 was identified with wild-type stature. It was twice backcrossed with a homozygous *cpr22* plant for genetic analysis.

Trypan blue staining

Leaf samples were taken from 2–3-week-old plants grown on soil. Trypan blue staining was performed as described previously (Yoshioka *et al.*, 2001).

RNA extraction and RT-PCR

Small-scale RNA extraction was carried out using the TRIzol reagent (Invitrogen, http://www.invitrogen.com/), according to the manufacturer's instructions. Reverse transcriptase-PCR was performed using cDNA generated by SuperScript® II Reverse Transcriptase (Invitrogen) according to the manufacturer's instructions. For the detection of CNGC gene expression in *N. benthamiana*, cDNA13-Fwd17: 5′-AGAAGGTTTACTGGAGG-3′ and F11C10-14-R3: 5′-GGAAGGCGAGAACCATT-3′ were used. For the detection of CNGC gene expression in yeast, cDNA13-F1:5′-AGGTTTACTG GAGGAAGACC-3′ and cDNA14-R1: 5′-CAC TATGCTTCAGCCTTTGC-3′ were used. For the detection of actin expression in yeast, ACT_fwd 5′-CCTACGTTGGTGATGAAGCT-3′ and ACT_rev, 5′-GTC AGTCAAATCTCTACCGG-3′ were used. For the detection of β-tubulin in Arabidopsis, β-tubulin_fwd:5′-CGTGGATCACAGCAATACA-GAGCC-3 and β-tubulin_rev: 5′-CCTCCTGCACTTCCACTTCGTCTTC-

3′ were used. Cycle conditions in each analysis are listed in the figure legends.

Pathogen infection

Infection with *H. parasitica* isolates Emwa1 was performed as described previously (Yoshioka *et al.*, 2001).

Plasmid construction

AtCNGC11/12 cDNA minus the stop codon, fused with GFP (smGFP) in pMBP3 (Urquhart *et al.*, 2007; Yoshioka *et al.*, 2006) was excised using *Xho*I and subsequently subcloned into pBluescript (Stratagene, http://www.stratagene.com/). The #73 point mutation E519K (G1555A) was introduced into this *AtCNGC11/12* cDNA in pBluescript using the QuickChange site-directed mutagenesis kit (Stratagene) according to the manufacturer's instructions. The *AtCNGC11/12:E519K* cDNA was sequenced and subcloned back into pMBP3.

The plasmid pYES2 (Invitrogen), pYES2-AtCNGC12 and pYES2-AtCNGC11/12 pYES2-AtCNGC11/12:*E519K* were constructed as previously described (Yoshioka *et al.*, 2006). For the construction of pYES2-*AtCNGC12*:*E527K*, pYES2-*AtCNGC11/12:E519K* and pYES2-*AtCNGC12* were digested by *Mun*I and *Xba*I. The fragment from pYES2-*AtCNGC11/12-E519K* which contains the *E519K* mutation was ligated into digested pYES2-*AtCNGC12.* All constructed plasmids were sequenced for fidelity.

Agrobacterium-*mediated transient expression*

Agrobacterium-mediated transient expression in *N. benthamiana* was performed as described in Urquhart *et al.* (2007). The expression of these genes was confirmed by RT-PCR (see 'RNA extraction and RT-PCR').

Functional characterization of CNGCs in yeast

The K^+-uptake-deficient yeast mutant strain CY162 (MAT α, ura3-52, *trk1,2*) was provided by Dr L. Kochian (Cornell University, Ithaca, NY, USA). The CY162 was transformed with the empty plasmid pYES2, pYES2-*AtCNGC12*, pYES2-*AtCNGC11/12*, pYES2-*AtCNGC11/12:E519K*, pYES2-*AtCNGC12:E527K* and pYES2-*AtCNGC11/12:R384I* following the lithium acetate transformation protocol (Ausubel *et al.*, 1987). Complementation analysis was conducted as previously described (Leng *et al.*, 1999) with the modification of the addition of hygromycin (5 mg l^{-1}) to suppress the background (Ali *et al.*, 2005; Mercier *et al.*, 2004).

Subcellular localization analysis

Protoplast isolation and transfection with 10 μg of plasmid pMBP3-*AtCNGC12:GFP*, pMBP3-*AtCNCG11/12:GFP*, pMBP3- *AtCNGC11/12:E519K:GFP*, pMBP3-*GFP* or a plasmid which expresses a plasma membrane-localized protein, *SYP123:GFP*, was performed as described in Fujikawa and Kato (2007). No plasmid was added during the transfection procedure to the mock samples.

Protein expression in E. coli

The portions from the beginning of the CNBD to the end of the cytosolic C-terminal region (T1298-G1905) of AtCNGC11/12 cDNA and AtCNGC11/12:E519K cDNA were subcloned into the *Eco*RI–*Xho*I sites in the *E. coli* expression vector pET28a (Novagen, http://www.emdbiosciences.com/html/NVG/home.html) under the control of the T7 promoter with a His tag. All vectors were sequenced for confirmation and transformed into the *E. coli* strain BL21 (DE3). Protein expression in BL21 cells was induced by the addition of 1 mM isopropyl β-D-1-thiogalactopyranoside (IPTG) and the cells were grown overnight at 16°C. Proteins were extracted in lysis buffer [150 mM NaCl, 0.5% NP40, 5 mM EDTA pH 5.0 and 10 mM 2-amino-2-(hydroxymethyl)-1,3-propanediol (TRIS) pH 7.5] by sonication. Subsequently His-tagged proteins were purified using nickel-nitrilotriacetic acid (Ni-NTA) affinity chromatography. Fractions were pooled together and dialyzed overnight at 4°C in 50 mM TRIS pH 7.5, 150 mM KCl, 5 mM $MgCl_2$ and 1 mM DTT.

In vitro *cAMP binding assay*

Agarose beads coated with cAMP (Sigma) were resuspended in 1 ml buffer (50 mM TRIS pH 7.5, 150 mM KCl, 5 mM $MgCl_2$ and 1 mM DTT) and 50 μl of this resin was incubated with 250 μg of either purified protein CNBD12, CNBD11/12:E519K or aconitase for 20 min at 4°C. The beads were briefly spun down and the flow-through was collected. The beads were then washed three times with the CNBD assay buffer containing 500 mM NaCl. The beads were then mixed with 50–100 μl of 2× SDS-loading buffer and boiled for 5 min. The samples were run on a 12% SDS-PAGE gel and used for Western blotting to detect the protein with an α-His-tag antibody.

Western blot analysis

For detection of the His-tagged proteins, protein extracts were separated by SDS-PAGE, blotted onto a PVDF membrane (Millipore, http://www.millipore.com/) and probed with an α-His antibody (1:2000 dilution; BioShop, http://www.bioshopcanada.com/) and then with an α-mouse antibody conjugated to horseradish peroxidase (1:2000 dilution; Cell Signaling, http://www.cst.neb.com/). Chemiluminescence was detected using the Western Lightning reagent Plus (PerkinElmer, http://www.perkinelmer.com/) following the manufacturer's protocol.

Computational modeling and sequence alignment

To address the secondary and tertiary structure of AtCNGC11/12 the secondary structure prediction tool PHYRE (McDonnell *et al.*, 2006; www.sbg.bio.ic.ac.uk/phyre/html/index.html) was used. A multiple sequence alignment of 14 homologous sequences was generated through ProbCons (Do *et al.*, 2005) and was edited manually to obtain the best possible alignment for modeling. A pairwise alignment of the cytosolic C-terminus domain from AtCNGC11/12 (same as AtCNGC12) of ecotype Wassilewskija (accession EU541495) to the sequence of the crystallized structure of the cytoplasmic C-terminus of HCN2 (PDB# 1Q50) was extracted from the final multiple sequence alignment above, and was used to generate the homology models through SWISSMODEL (Schwede *et al.*, 2003). The same portion was also modeled to the crystallized structure of the CNBD from RIα (PDB# 1NE6). All the images were generated using PyMOL (DeLano, 2002).

The sequence alignments of the CNBD amino acid sequences of all 20 Arabidopsis putative CNGCs were aligned using CLUSTALW (Thompson *et al.*, 1994). The accession numbers of protein sequence of CNGCs and other ion channels used for multiple sequence alignment as well as computational modeling are as indicated in the table and figure legends.

Acknowledgements

We thank Dr L. Kochian at Cornell University for providing the CY162 yeast strain. We would like to thank Dr Y. Chong, Dr W. Ckurshumova, Mr H. Hong and Dr D. Gupta for technical assistance. We also thank Dr M. H. Sato for GFP-SYP123. This work was supported by a Discovery grant of the Natural Science and Engineering Research Council of Canada, Canadian Foundation for Innovation, the Ontario Research Fund and the Early Researcher Award of the Ontario Ministry of Research and Innovation to KY and Graduate Scholarship of the Natural Science and Engineering Research Council of Canada to WU.

Supporting Information

Additional Supporting Information may be found in the online version of this article:

Figure S1. The PCR-based marker analysis for *cpr22* homozygosity.

Figure S2. Detection of *AtCNGC12*, *AtCNGC11/12*, *AtCNGC11/12:E519K*, *AtCNGC12:E527K* and *AtCNGC11/12:R384R* by semi-quantitative RT-PCR analysis in yeast CY162.

Please note: Wiley-Blackwell are not responsible for the content or functionality of any supporting materials supplied by the authors. Any queries (other than missing material) should be directed to the corresponding author for the article.

References

Ali, R., Zielinski, E.R. and Berkowitz, G.A. (2005) Expression of plant cyclic nucleotide-gated cation channels in yeast. *J. Exp. Bot.* **57**, 125–138.

Ali, R., Ma, W., Lemtiri-Chlieh, F., Tsaltas, D., Leng, Q., von Bodman, S. and Berkowitz, G.A. (2007) Death don't have no mercy and neither does calcium: Arabidopsis CYCLIC NUCLEOTIDE GATED CHANNEL2 and innate immunity. *Plant Cell*, **19**, 1081–1095.

Arazi, T., Sunkar, R., Kaplan, B. and Fromm, H. (1999) A tobacco plasma membrane calmodulin-binding transporter confers Ni^{2+} tolerance and Pb^{2+} hypersensitivity in transgenic plants. *Plant J.* **20**, 171–182.

Ausubel, F.M., Bent, R., Kingston, R.E., Moore, D.D., Seidman, J.G., Smith, J.A. and Struhl, K. (1987) *Current Protocols in Molecular Biology*. New York: John Wiley & Sons.

Balague, C., Lin, B., Alcon, C., Flottes, G., Malmstrom, S., Köhler, C., Neuhaus, G., Pelletier, G., Gaymard, F. and Roby, D. (2003) HLM1, an essential signaling component in the hypersensitive response, is a member of the cyclic nucleotide-gated channel ion channel family. *Plant Cell*, **15**, 365–379.

Biel, M., Seeliger, M., Pfeifer, A., Kohler, K., Gerstner, A., Ludwig, A., Jaissle, G., Fauser, S., Zrenner, E. and Hofmann, F. (1999) Selective loss of of cone function in mice lacking the cyclic nucleotide-gated channel CNG3. *Proc. Natl Acad. Sci. USA*, **96**, 7553–7557.

Borsics, T., Webb, D., Andeme-Ondzighi, C., Staehelin, L.A. and Christopher, D.A. (2007) The cyclic nucleotide-gated calmodulin-binding channel AtCNGC10 localizes to the plasma membrane and influences numerous growth responses and starch accumulation in *Arabidopsis thaliana*. *Planta*, **225**, 563–573.

Bridges, D., Fraser, M.E. and Moorhead, G.B.G. (2005) Cyclic nucleotide binding proteins in the *Arabidopsis thaliana* and *Oryza sativa* genomes. *BMC Bioinformatics*, **11**, 6:6.

Chan, C.W.M., Schorrak, L.M., Smith, R.K., Bent, A.F. and Sussman, M.R. (2003) A cyclic nucleotide-gated ion channel, CNGC2, is crucial for plant development and adaptation to calcium stress. *Plant Physiol.*, **123**, 728–731.

Clough, S.J., Fengler, K.A., Yu, I.C., Lippok, B., Smith, R.K., Jr and Bent, A.F. (2000) The *Arabidopsis dnd1* ''defense, no death'' gene encodes a mutated cyclic nculeotide-gated ion channel. *Proc. Natl Acad. Sci. USA*, **97**, 9323–9328.

Craven, K.B. and Zagotta, W.N. (2004) Salt bridges and gating in the COOH-terminal region of HCN2 and CNGA1 channels. *J. Gen. Physiol.* **124**, 663–677.

DeLano, W.L. (2002) *The PyMOL Molecular Graphics System*. Palo Alto, CA: DeLano Scientific.

Do, C.B., Mahabhashyam, M.S.P., Brudno, M. and Batzoglou, S. (2005) PROBCONS: probabilistic consistency-based multiple sequence alignment. *Genome Res.* **15**, 330–340.

Durner, J., Wendehennne, D. and Klessig, D.F. (1998) Defense gene induction in tobacco by nitric oxide, cyclic GMP, and cyclic ADP-ribose. *Proc. Natl Acad. Sci. USA*, **95**, 10328–10333.

Fesenko, E.E., Kolesnikov, S.S. and Lyubarsky, A.L. (1985) Induction by cyclic GMP of cationic conductance in plasma membrane of retinal rod outer segment. *Nature*, **313**, 310–313.

Frietsch, S., Wang, Y.-F., Sladek, C., Poulsen, L.R., Romanowsky, S.M., Schroeder, J.I. and Harper, J.F. (2007) A cyclic nucleotide-gated channel is essential for polarized tip growth of pollen. *Proc. Natl Acad. Sci. USA*, **104**, 14531–14536.

Fujikawa, Y. and Kato, N. (2007) Split luciferase complementation assay to study protein-protein interactions in Arabidopsis protoplasts. *Plant J.* **52**, 185–195.

Gobert, A., Park, G., Amtmann, A., Sanders, D. and Maathuis, F.J. (2006) *Arabidopsis thaliana* cyclic nucleotide gated channel 3 forms a non-selective ion transporter involved in germination and cation transport. *J. Exp. Bot.* **57**, 791–800.

Goulding, E.H., Tibbs, G.R. and Siegelbaum, S.A. (1994) Molecular mechanism of cyclic-nucleotide-gated channel activation. *Nature*, **372**, 369–374.

Hua, B.-G., Mercier, R.W., Zielinski, R.E. and Berkowitz, G.A. (2003) Functional interaction of calmodulin with a plant cyclic nucleotide gated cation channel. *Plant Physiol. Biochem.* **41**, 945–954.

Jiang, J., Fan, L.W. and Wu, W.H. (2005) Evidences for involvement of endogenous cAMP in Arabidopsis defense responses to *Verticillium* toxins. *Cell Res.* **15**, 585–592.

Johnson, J.P., Jr and Zagotta, W.N. (2001) Rotational movement during cyclic nucleotide-gated channel opening. *Nature*, **412**, 917–921.

Jurkowski, G.I., Smith, R.K., Jr, Yu, I.C., Ham, J.H., Sharma, S.B., Klessig, D.F., Fengler, K.A. and Bent, A.F. (2004) Arabidopsis DND2, a second cyclic nucleotide-gated ion channel gene for which mutation causes the ''defense, no death'' phenotype. *Mol. Plant Microbe Interact.* **17**, 511–520.

Kaplan, B., Sherman, T. and Fromm, H. (2007) Cyclic nucleotide-gated channels in plants. *FEBS Lett.* **581**, 2237–2246.

Kaupp, U.B. and Seifert, R. (2002) Cyclic nucleotide-gated ion channels. *Physiol. Rev.* **82**, 769–824.

Köhler, C. and Neuhaus, G. (1998) Cloning and partial characterization of two putative cyclic nucleotide-regulated ion channels from *Arabidopsis thaliana*, designated CNGC1 (Y16327), CNGC2 (Y16328) (PGR98-062). *Plant Physiol.* **116**, 1604.

Köhler, C., Merkle, T. and Neuhaus, G. (1999) Characterization of a novel gene family of putative cyclic nucleotide- and calmodulin-regulated ion channels in *Arabidopsis thaliana*. *Plant J.* **18**, 97–104.

Köhler, C., Merkle, T., Roby, D. and Neuhaus, G. (2001) Developmentally regulated expression of cyclic nucleotide-gated ion channel from Arabidopsis indicates its involvement in programmed cell death. *Planta*, **213**, 327–332.

Leng, Q., Mercier, R.W., Yao, W. and Berkowitz, G.A. (1999) Cloning and first functional characterization of a plant cyclic nucleotide-gated cation channel. *Plant Physiol.* **121**, 753–761.

Li, X., Borsics, T., Harrington, H.M. and Christopher, D.A. (2005) *Arabidopsis* AtCNGC10 rescues potassium channel mutants of *E. coli*, yeast, and *Arabidopsis* and is regulated by calcium/calmodulin and cyclic GMP in *E. coli*. *Funct. Plant Biol.* **32**, 643–653.

Ma, W., Ali, R. and Berkowitz, G.A. (2006) Characterization of plant phenotypes associated with loss-of-function of AtCNGC1, a plant cyclic nucleotide gated cation channel. *Plant Physiol Biochem.* **44**, 494–505.

Mäser, P., Thomine, S., Schroeder, J.I. *et al.* (2001) Phylogenetic relationships within cation transporter families of *Arabidopsis*. *Plant Physiol.* **126**, 1646–1667.

McDonnell, A.V., Jiang, T., Keating, A.E. and Berger, B. (2006) Paircoil2: improved prediction of coiled coils from sequence. *Bioinformatics*, **22**, 356–358.

Mercier, R.W., Rabinowitz, N.M., Ali, R., Gaxiola, R.A. and Berkowitz, G.A. (2004) Yeast hygromycin sensitivity as a functional assay of cyclic nucleotide-gated cation channels. *Plant Physiol. Biochem.* **42**, 529–536.

Moeder, W., del Pozo, O., Navarre, D.A., Martin, G.B. and Klessig, D.F. (2007) Aconitase plays a role in regulating resistance to oxidative stress and cell death in Arabidopsis and *Nicotiana benthamiana*. *Plant Mol. Biol.* **63**, 273–287.

Moutinho, A., Hussey, P.J., Trewavas, A.J. and Malho, R. (2001) cAMP acts as a second messenger in pollen tube growth and reorientation. *Proc. Natl Acad. Sci. USA*, **98**, 10481–10486.

Newton, R.P. and Smith, C.J. (2004) Molecules of interest; cyclic nucleotides. *Phytochemistry*, **65**, 2423–2437.

Pagnussat, G.C., Lanteri, M.L. and Lamattina, L. (2003) Nitric oxide and cyclic GMP are messengers in the indole acetic acid-induced adventitious rooting process. *Plant Physiol.* **132**, 1241–1248.

Rall, T.W., Sutherland, E.W. and Berthet, L. (1957) The relation of epinephrine and glucagon to liver phosphorylase. *J. Biol. Chem.* **224**, 1987–1995.

Rostoks, N., Schmierer, D., Mudie, S., Drader, T., Brueggeman, R., Caldwell, D.G., Waugh, R. and Kleinhofs, A. (2006) Barley necrotic locus nec1 encodes the cyclic nucleotide-gated ion channel 4 homologous to the Arabidopsis HLM1. *Mol. Genet. Genomics*, **275**, 159–168.

Schuurink, R.C., Shartzer, S.F., Fath, A. and Jones, R.L. (1998) Characterization of a calmodulin-binding transporter from the plasma membrane of barley aleurone. *Proc. Natl Acad. Sci. USA*, **95**, 1944–1949.

Schwede, T., Kopp, J., Guex, N. and Peitsch, M.C. (2003) SWISS-MODEL: an automated protein homology-modeling server. *Nucleic Acids Res.* **31**, 3381–3385.

Silva, H., Yoshioka, K., Dooner, H.K. and Klessig, D.F. (1999) Characterization of a new Arabidopsis mutant exhibiting enhanced disease resistance. *Mol. Plant Microbe Interact.* **12**, 1053–1063.

Sunkar, R., Kaplan, B., Bouche, N., Arazi, T., Dolev, D., Talke, I.N., Maathuis, F.J., Sanders, D., Bouchez, D. and Fromm, H. (2000) Expression of a truncated tobacco NtCBP4 channel in transgenic plants and disruption of the homologous Arabidopsis CNGC1 gene confer $Pb2^{+}$ tolerance. *Plant J.* **24**, 533–542.

Talke, I.N., Blaudez, D., Maathuis, F.J.M. and Sanders, D. (2003) CNGCs: prime targets of plant cyclic nucleotide signaling? *Trends Plant Sci.* **8**, 286–293.

Thompson, J.D., Higgins, D.G. and Gibson, T.J. (1994) CLUSTAL W: improving the sensitivity of progressive multiple sequence alignment through sequence weighting, position specific gap penalties and weight matrix choice. *Nucleic Acids Res.* **22**, 4673–4680.

Uemura, T., Ueda, T., Ohniwa, R.L., Nakano, A., Takeyasu, K. and Sato, M.H. (2004) Systematic analysis of SNARE molecules in Arabidopsis: dissection of the post-Golgi network in plant cells. *Cell Struct. Funct.* **29**, 49–65.

Urquhart, W., Gunawardena, A.H.L.A.N., Moeder, W., Ali, R., Berkowitz, G.A. and Yoshioka, K. (2007) The chimeric cyclic nucleotide-gated ion channel ATCNGC11/12 constitutively induces programmed cell death in a Ca^{2+} dependent manner. *Plant Mol. Biol.* **65**, 747–761.

Wissinger, B., Gamer, D., Jägle, H. *et al.* (2001) *CNGA3* mutations in hereditary cone photoreceptor disorders. *Am. J. Hum. Genet.* **69**, 722–733.

Yoshioka, K., Kachroo, P., Tsui, F., Sharma, S.B., Shah, J. and Klessig, D.F. (2001) Environmentally-sensitive, SA-dependent defense response in the *cpr22* mutant of *Arabidopsis*. *Plant J.* **26**, 447–459.

Yoshioka, K., Moeder, W., Kang, H.G., Kachroo, P., Masmoudi, K., Berkowitz, G. and Klessig, D.F. (2006) The chimeric Arabidopsis CYCLIC NUCLEOTIDE-GATED ION CHANNEL11/12 activates multiple pathogen resistance responses. *Plant Cell*, **18**, 747–763.

Zagotta, W.N. and Siegelbaum, S.A. (1996) Structure and function of cyclic nucleotide-gated channels. *Annu. Rev. Neurosci.* **19**, 235–263.

Zagotta, W.N., Olivier, N.B., Black, K.D., Young, E.C., Olson, R. and Gouaux, E. (2003) Structural basis for modulation and agonist specificity of HCN pacemaker channels. *Nature*, **425**, 200–205.

Zhong, H., Lai, J. and Yau, K.W. (2003) Selective heteromeric assembly of cyclic nucleotide-gated channels. *Proc. Natl Acad. Sci. USA*, **100**, 5509–5513.

Zufall, F., Firestein, S. and Shepherd, G.M. (1994) Cyclic nucleotide-gated ion channels and sensory transduction in olfactory receptor neurons. *Annu. Rev. Biophys. Biomol. Struct.* **23**, 577–607.

